Turbulent burning velocity and thermodiffusive instability of premixed flames

Hsu Chew Lee,[1,2] B. Wu,[1] Peng Dai,[1] Minping Wan,[1,2,3,*] and Andrei N. Lipatnikov[4,†]

[1]*Guangdong Provincial Key Laboratory of Turbulence Research and Applications, Department of Mechanics and Aerospace Engineering, Southern University of Science and Technology, Shenzhen 518055, People's Republic of China*

[2]*Guangdong-Hong Kong-Macao Joint Laboratory for Data-Driven Fluid Mechanics and Engineering Applications, Southern University of Science and Technology, Shenzhen 518055, People's Republic of China*

[3]*Jiaxing Research Institute, Southern University of Science and Technology, Jiaxing, 314031, Zhejiang, People's Republic of China*

[4]*Department of Mechanics and Maritime Sciences, Chalmers University of Technology, Göteborg, 412 96, Sweden*

(Received 26 February 2023; accepted 2 August 2023; published 1 September 2023)

Reported in the paper are results of unsteady three-dimensional direct numerical simulations of laminar and turbulent, lean hydrogen-air, complex-chemistry flames propagating in forced turbulence in a box. To explore the eventual influence of thermodiffusive instability of laminar flames on turbulent burning velocity, (i) a critical length scale Λ_n that bounds regimes of unstable and stable laminar combustion is numerically determined by gradually decreasing the width Λ of computational domain until a stable laminar flame is obtained, and (ii) simulations of turbulent flames are performed by varying the width from $\Lambda < \Lambda_n$ (in this case, the instability is suppressed) to $\Lambda > \Lambda_n$ (in this case, the instability may grow). Moreover, simulations are performed either using mixture-averaged transport properties (low Lewis number flames) or setting diffusivities of all species equal to heat diffusivity of the mixture (equidiffusive flames), with all other things being equal. Obtained results show a significant increase in turbulent burning velocity U_T when the boundary $\Lambda = \Lambda_n$ is crossed in weak turbulence, but almost equal values of U_T are computed at $\Lambda < \Lambda_n$ and $\Lambda > \Lambda_n$ in moderately turbulent flames characterized by a Karlovitz number equal to 3.4 or larger. These results imply that thermodiffusive instability of laminar premixed flames substantially affects burning velocity in weak turbulence only, in line with a simple criterion proposed by Chomiak and Lipatnikov (Phys. Rev. E **107**, 015102, (2023)).

DOI: 10.1103/PhysRevE.108.035101

I. INTRODUCTION

Since premixed turbulent combustion is a multiscale and highly nonlinear phenomenon [1], it involves a variety of local effects, reviewed elsewhere [2–6], with these effects significantly enriching the physics of turbulent reacting flows. In particular, the rate of premixed combustion is known to be increased not only by a wide spectrum of turbulent velocity fluctuations [7–10], but also by hydrodynamic (Darrieus-Landau, DL) and thermodiffusive (TD) instabilities of laminar flames[1] [11–16], with the interactions between turbulence and flame instabilities still challenging the combustion community. This fundamental challenge has also been attracting rapidly growing interest in applied computational fluid dynamics (CFD) research aimed at developing zero-emission technologies for power generation by utilizing chemical energy bound in renewable carbon-free fuels such as hydrogen. The point is that (i) since pioneering experiments by Karpov *et al.* [17,18], significant differences between molecular diffusivities of H_2, O_2, and heat were well known to result in strongly increasing turbulent burning velocities U_T in sufficiently lean hydrogen-air mixtures, as reviewed elsewhere [8,16,19], see also recent experimental studies [20–22]; (ii) a similar phenomenon was also documented in experiments with fuel blends that contain H_2, e.g., lean syngas/air mixtures [23–26] or lean ammonia/hydrogen/air mixtures [27–31]; (iii) a widely established predictive model of this important effect has yet to be developed, while (iv) the effect is often discussed [16,21,27,30,32–37] in terms of TD instability of laminar premixed flames.

Indeed, on the one hand, both the increase in U_T and TD instability result from variations in local burning rate, caused by differential diffusion effects, i.e., local variations in temperature and reactant concentrations due to imbalance of molecular fluxes of thermal and chemical energies from and to, respectively, reaction zones stretched by the local velocity field [3,8,11,38]. This similarity of the governing physical mechanisms encourages researchers to link the two phenomena. However, on the other hand, the present authors are not aware of convincing evidence that the increase in U_T stems from local instabilities of inherently laminar flames

*wanmp@sustech.edu.cn

†andrei.lipatnikov@chalmers.se

[1]While hydrodynamic instability can arise in any premixed flame characterized by a finite density drop from the unburned side to the burned side, thermodiffusive instability can only arise in mixtures characterized by a low Lewis number $Le < 1$ [11], which is equal to a ratio of molecular mass diffusivity of deficient reactant to molecular heat diffusivity of the mixture. Accordingly, a premixed laminar flame characterized by a low Le is subject to both instabilities. Henceforth, the term "DL instability" refers to hydrodynamic instability of a laminar flame characterized by $Le \geqslant 1$, whereas the term "TD instability" refers to joint effects of both hydrodynamic and thermodiffusive instabilities on a laminar flame characterized by a low $Le < 1$, as the latter effect is stronger.

in a turbulent flow. Specifically, the present authors are not aware of a model that predicts the increase magnitude by invoking characteristics of TD instability, such as, e.g., its growth rate. On the contrary, a high magnitude of an increase in U_T in lean hydrogen flames was computed [19,39] adopting another approach, which disregarded TD instability, but, following the leading point concept of premixed turbulent combustion [8,11], highlighted local variations in temperature, reactant concentrations, and burning rate in highly stretched reaction zones localized to the leading edge of a premixed flame brush. A summary of recent developments in that research direction will be provided in the end of Sec. III.

Moreover, the following simple order-of-magnitude criterion

$$Ka = \frac{\tau_f}{\tau_K} < Ka_{TD}^{cr} = \sqrt{15}\tau_f \max\{\omega_{TD}(k)\} \qquad (1)$$

of importance of TD instability in turbulent flows has recently been introduced [40] by highlighting mitigation of flame instabilities by normal flame strain rates [41–43], which are created by small-scale eddies in turbulent flows. Here, Ka is a Karlovitz number; $\tau_f = \delta_L/S_L$, S_L, and $\delta_L = (T_b - T_u)/\max\{|dT/dx|\}$ are the laminar flame time scale, speed, and thickness, respectively; T is the temperature; subscripts u and b designate unburned reactants and burned products; $\max\{\omega_{TD}(k)\}$ is the maximum growth rate of TD instability (dependence of the instability growth rate ω_{TD} on the instability wave number k has a bell-shape form [44–49], as discussed in the next section); and τ_K is Kolmogorov time scale, which characterizes the order of magnitude of the highest velocity gradients generated by the smallest-scale turbulent eddies [12,50,51]. Similar criteria of importance of DL instability in turbulent flows were earlier introduced using the same reasoning [19], as well as other reasoning [52,53], and results of subsequent numerical [54–57] and experimental [58,59] studies qualitatively supported those criteria by indicating a minor role played by DL instability under conditions of sufficiently intense turbulence.

However, a role played by TD instability of laminar premixed flames in turbulent flows is still an intricate fundamental and practically important issue. The present paper aims at clarifying it by reporting results of a target-directed direct numerical simulation (DNS) study. In the next section, the adopted research method is presented and the DNS attributes are summarized. Obtained results are discussed in Sec. III, followed by conclusions.

II. METHOD

A. Key point

The present work is based on a seminal idea put forward and developed recently by Matalon *et al.* [54–57] who numerically studied interactions of DL instability with turbulence. This idea stems from the following considerations. Both theoretical [60–64] and experimental [65,66] studies of DL instability show that dependence of the instability growth rate ω_{DL} on perturbation wave number k has a bell-shape form, see Fig. 1, i.e., a peak growth rate $\omega_{DL} > 0$ is reached at certain wave number k_m, whereas molecular transport processes stabilize the flame with respect to small-scale

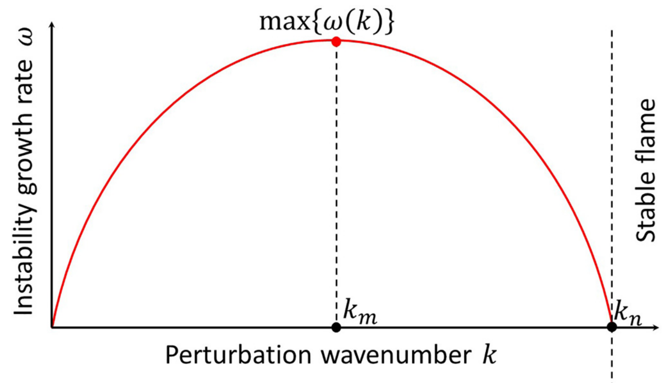

FIG. 1. A typical dispersion relation for unstable laminar premixed flame.

perturbations whose wave number is larger than the neutral wave number k_n, with $k_n \approx 2k_m$ and $\omega_{DL}(k > k_n) < 0$. Accordingly, variations in a computational domain width Λ offer the opportunity to numerically explore a role played by DL instability in premixed turbulent combustion by comparing results simulated under conditions of $\Lambda < \Lambda_n = 2\pi/k_n$ (the instability is suppressed) and $\Lambda > \Lambda_n$ (the instability can grow), with all other things being equal. Results obtained in such simulations [54–57] showed that DL instability could substantially contribute to U_T under conditions of weak turbulence only, in line with simple phenomenological criteria proposed earlier [19,52,53].

Recent two-dimensional numerical simulations of laminar premixed flames subject to TD instability [44–49] have shown that $\omega_{TD}(k)$ has a bell-shape form also, with $\omega_{TD}(k = k_m) = \max\{\omega_{TD}(k)\} > 0$, $\omega_{TD}(k > k_n) < 0$, and $k_n \approx 2k_m$. Therefore, the influence of TD instability on turbulent burning velocity may be explored by comparing DNS results obtained in the cases of $\Lambda < \Lambda_n = 2\pi/k_n$ (the instability is suppressed) and $\Lambda > \Lambda_n$ (the instability can grow), with all other things being equal.

This approach is implemented in the present work by simulating lean (the equivalence ratio $\phi = 0.5$) complex-chemistry hydrogen-air flames propagating under room conditions either in a laminar flow or in forced turbulence in a box. It is worth stressing, however, that the primary goal of the present study calls for specific conditions of the performed DNSs.

First, since (i) the study aims at comparing results computed in domains whose widths are comparable with (slightly smaller and slightly larger than) Λ_n and (ii) Λ_n is sufficiently small for the adopted mixture, see Sec. II.C, the DNSs should be run in narrow computational domains, significantly narrower than computational domains used in a typical DNS study of a complex-chemistry turbulent premixed flame. Accordingly, the present work does not aim at exploring evolution of TD instability in a laminar or turbulent flow, because much wider computational domains are known to be required to numerically predict major characteristics of a nonlinear stage of the growth of a laminar flame instability [67–69]. As the present work aims solely at investigating eventual suppression of TD instability by turbulence, the focus of the study is placed on the onset (if any) of the instability in various turbulent flows.

TABLE I. Characteristics of DNS cases.

Case	S_L, m/s	δ_L, mm	u'/S_L	L/δ_L	Re_λ	Ka	Da	$\Delta x/L$	$\Delta x/\eta_K$	N	Λ mm	$\overline{U_T}/S_L$
LT/S	0.58	0.41	0.34	0.58	7.9	0.9	1.8	0.08	0.21	64	1.26	1.05
LT/U	0.58	0.41	0.34	0.61	7.5	0.9	1.8	0.08	0.22	64	1.32	1.64
WT/U	0.58	0.41	0.50	0.61	9.8	1.6	1.2	0.08	0.30	64	1.32	1.71
T/S	0.58	0.41	1.0	0.58	13.7	4.4	0.6	0.04	0.24	128	1.26	1.90
T/U	0.58	0.41	1.0	0.61	14.0	4.3	0.6	0.04	0.25	128	1.32	1.93
T/UM	0.58	0.41	1.0	1.1	18.0	3.4	1.1	0.04	0.40	128	2.4	3.29
T/U1	0.78	0.29	0.74	0.61	14.7	2.2	1.2	0.04	0.24	128	1.32	1.10
T/UM1	0.78	0.29	0.74	1.1	18.0	1.8	2.1	0.04	0.40	128	2.4	1.73

Second, as discussed in Sec. III, TD instability is suppressed by moderately intense turbulence characterized by $Ka > Ka_{TD}^{cr}$, where the critical value is $1.6 < Ka_{TD}^{cr} < 3.4$ for the studied mixture. Since the restriction on the computational domain width, highlighted above, requires considering small-scale turbulence (its integral length scale L should be significantly less than the width Λ) and $Ka \propto (u'/S_L)^{3/2}(L/\delta_L)^{-1/2}$, this critical value Ka_{TD}^{cr} can be reached at sufficiently low rms turbulent velocities u'. Such a weak and small-scale turbulence is characterized by a sufficiently low Reynolds number and even the use of the word "turbulence" may be disputed, e.g., due to the lack of the inertial range of turbulence spectrum. Nevertheless, such unusual conditions may still be appropriate for the major goal of the present study. Indeed, if such weak turbulence can suppress TD instability, as will be shown in Sec. III, there is no reason to expect that the instability could arise in more intense turbulence characterized by a higher Ka. If TD instability can play a role in weakly and moderately turbulent flames only, running DNS of highly turbulent flames to explore TD instability effects does not seem to be a worthy task.

Thus, when the present DNS study was started, its conditions were set using a constraint of $\Lambda \approx \Lambda_n$ and Eq. (1). Since the computed results agreed with Eq. (1) to the leading order, there was no need for running DNS by increasing u'/S_L, especially as DNS results obtained recently from highly turbulent flames propagating in wider boxes were already reported by us [70–77].

B. DNS attributes

Since the present DNSs are basically similar to our simulations discussed in detail earlier [70–77], only a summary of the DNS attributes is given below.

Unsteady three-dimensional simulations of statistically one-dimensional and planar flames propagating under room conditions in forced turbulence (or a laminar flow) in a box were performed using a detailed chemical mechanism (9 species and 22 reversible reactions) by Kéromnès *et al.* [78], with mixture-averaged molecular transport and chemical reaction rates being modeled using open-source library Cantera-2.3 [79]. Navier-Stokes, energy, and species transport equations written in the low-Mach-number formulation were numerically integrated using solver DINO [80]. It adopts a sixth-order finite-difference central stencil and a semi-implicit third-order Runge-Kutta method for time advancement.

A rectangular computational domain of $16\Lambda \times \Lambda \times \Lambda$ was discretized using a uniform Cartesian grid of $16N \times N \times N$ cells. The adopted numerical meshes ensured more than 20 grid points across the thickness δ_L in the majority of the studied cases, while the number of grid points per δ_L was less (15) in two equidiffusive flames discussed later. In all cases, half the Kolmogorov length scale η_K was larger than the grid size Δx, see Table I. Along the streamwise direction x, inflow and outflow boundary conditions were set. Other boundary conditions were periodic.

Within a rectangular domain of $0.5\Lambda \leqslant x \leqslant 8\Lambda$, turbulence was generated using the linear velocity forcing method [81–83] and the evolution of this turbulence was simulated for at least 50 integral time scales $\tau_t = L/u'$ before embedding the steady planar laminar flame solution obtained using Cantera-2.3 [79] in the computational domain. Here, $u' = \overline{\langle u_i' u_i' \rangle}/3$ is rms turbulent velocity; the integral length scale $L = {u_0'}^3/\overline{\langle \varepsilon \rangle}_0$ yielded by the adopted forcing method is about 0.19Λ [81–83]; $\varepsilon = 2\nu S_{ij} S_{ij}$ is the dissipation rate of turbulent kinetic energy; ν is the kinematic viscosity of the mixture; $S_{ij} = (\partial u_i/\partial x_j + \partial u_j/\partial x_i)/2$ is rate-of-strain tensor; u_i is ith component of velocity vector; overline and angle brackets refer to time and transverse-averaged quantities, respectively; summation convention applies to repeated indexes (i or j); and subscript 0 refers to the constant-density nonreacting turbulent flow simulated before embedding the flame into the computational domain. In turbulent flame brush, u' varies weakly, while $\overline{\langle \varepsilon \rangle}$ increases gradually along the axial direction [72]. The combustion simulations were run for at least $30\tau_t$.

C. DNS conditions

The simulation conditions are summarized in Table I, where $Re_\lambda = u'\lambda/\nu$ is the turbulent Reynolds number based on the Taylor length scale $\lambda = u'(15\nu/\overline{\langle \varepsilon \rangle})^{1/2}$; $Ka = \tau_f/\tau_K$ and $Da = \tau_t/\tau_f$ are turbulent Karlovitz and Damköhler numbers, respectively; $\eta_K = (\nu^3/\overline{\langle \varepsilon \rangle})^{1/4}$ and $\tau_K = (\nu/\overline{\langle \varepsilon \rangle})^{1/2}$ are Kolmogorov length and time scales, respectively, with the time and transverse-averaged dissipation rate $\overline{\langle \varepsilon \rangle}$ being averaged over flame-brush leading edge characterized by $\langle c_F \rangle (x,t) = 0.01$; $c_F = 1 - Y_F/Y_{F,u}$ designates combustion progress variable evaluated using the fuel mass fraction Y_F; and $\Delta x = \Lambda/N$ is the grid size. Reported in the last column

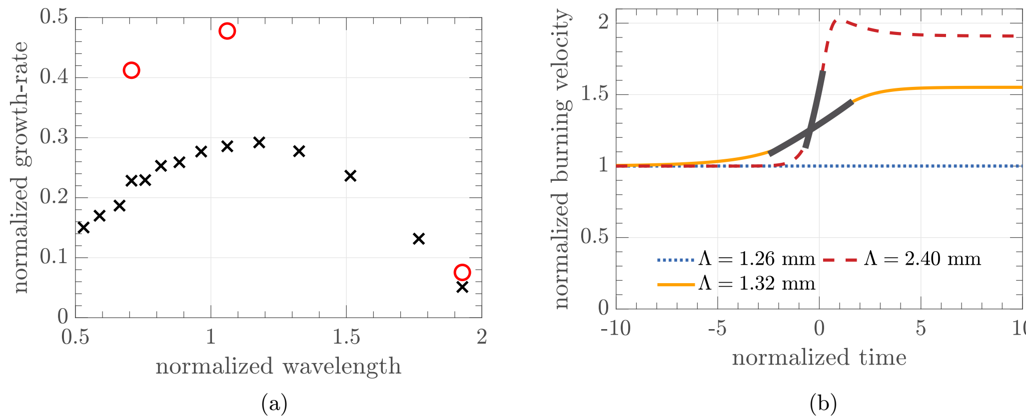

FIG. 2. (*a*) Normalized instability growth rates $\tau_f \omega_{TD}(k)$ obtained from two-dimensional (black crosses) and three-dimensional (red circles) laminar flames by varying the width Λ of the computational domain and the perturbation wave length $k = 2\pi/\Lambda$, with all other things being equal. (*b*) Normalized laminar burning velocities computed by varying Λ and $k = 2\pi/\Lambda$. In two unstable cases, the normalized time t/τ_f is shifted to get the maximum rate of an increase in the burning velocity at $t' = 0$. To evaluate the instability growth rate, the ordinate axis is scaled in the natural-logarithm units and thick black straight lines fit the computed curves.

are normalized time-averaged values of turbulent burning velocities, which have been evaluated by integrating the fuel consumption rate $\dot{\omega}_{H_2}(\boldsymbol{x}, t)$ over the computational domain, i.e.,

$$U_T(t) = \frac{1}{(\rho Y_{H_2})_u \Lambda^2} \iiint |\dot{\omega}_{H_2}|(\boldsymbol{x}, t) d\boldsymbol{x}. \quad (2)$$

Here, ρ is the density.

When compared to our earlier simulations [70,72], three differences should be emphasized. First, the rms velocity u' was reduced, because TD instability was assumed to be suppressed in highly turbulent flames and this assumption was supported in subsequent simulations, as discussed in Sec. III. Accordingly, letters LT, WT, and T in case names in Table I refer to transition from laminar to turbulent flows, weak turbulence, and moderately turbulent flames, respectively.

Second, the domain width Λ was varied from $\Lambda < \Lambda_n$ to $\Lambda > \Lambda_n$, with the neutral width Λ_n being found in pre-simulations of two-dimensional and three-dimensional laminar flames. In the two-dimensional case, Λ was changed with a small step, and weak periodic velocity perturbations with the wave number $k = 2\pi/\Lambda$ were generated at the inlet. Those presimulations were run adopting the same chemical and molecular transport models, the same solver, and $N = 128$, with the independence of the numerical results on the spatial resolution being checked using $N = 256$ or 512. Subsequently, these results were adopted to set conditions of a few three-dimensional presimulations, which were performed to find Λ_n in the three-dimensional case.

The results of these presimulations, reported in Fig. 2, see also Figs. 4(a) and 4(b) in the next section, show that the laminar flame is stable at $\Lambda = 1.26$ mm, but unstable at $\Lambda = 1.32$ mm, both in the two-dimensional and three-dimensional cases. For instance, instability growth rates computed in the two-dimensional and three-dimensional cases are plotted in black crosses and red circles, respectively, in Fig. 2(a). As illustrated in Fig. 2(b), these growth rates have been evaluated by (i) computing laminar burning velocities adapting Eq. (2) and (ii) fitting the linear parts of the obtained dependencies of $\ln(U_L/S_L)$ on time with straight lines. Dispersion relations $\omega(k)$ similar to the curve plotted in black crosses in Fig. 2(a) are well known from theoretical [60–64] and experimental [65,66] studies of DL instability, as well as from recent two-dimensional numerical simulations of thermodiffusively unstable laminar flames [44–49]. At large t/τ_f, a nonlinear stage of instability development, characterized by a quasistationary value of $\ln(U_L/S_L)$, is reached, see Fig. 2(b). This quasistationary value of $\ln(U_L/S_L)$ depends on the computational domain width Λ. Such a nonlinear stage was already investigated in recent two-dimensional numerical simulations [68,69] performed using significantly wider computational domains and, therefore, is beyond the scope of the present study, whose focus is solely placed on the onset of TD instability.

Based on the presented results of the laminar flame presimulations, letters S or U in case names in Table I refer to $\Lambda = 1.26$ mm (TD instability cannot arise, stable case) and $\Lambda = 1.32$ mm (the instability may occur, unstable case), respectively. The major goal of the present study is to compare turbulent burning velocities U_T computed in LT/S and LT/U or T/S and T/U cases.

Third, if Λ is slightly above Λ_n, the growth rate $\omega_{TD}(k)$ of allowed unstable perturbations is low, see Fig. 2(a), or compare the maximum slopes of curves plotted in yellow solid and red dashed lines in Fig. 2(b). Therefore, even if TD instability with respect to such perturbations is of minor importance when compared to turbulence, perturbations with the maximum growth rate $\omega_{TD}(k_m)$ might significantly affect turbulent burning velocity. To explore such a scenario, the width Λ was increased to 2.4 mm, i.e., by a factor of about two when compared to Λ_n. In this case, TUM, labeled with extra letter M in Table I, appearance of perturbations whose growth rates were close to $\max\{\omega_{TD}(k)\}$ was enabled, see the highest circle in Fig. 2(a).

However, the aforementioned increase in Λ can increase U_T not only due to development of TD instability, but also due to an increase in the turbulence length scale L (recall that $L = 0.19\Lambda$ under conditions of the present DNS), because

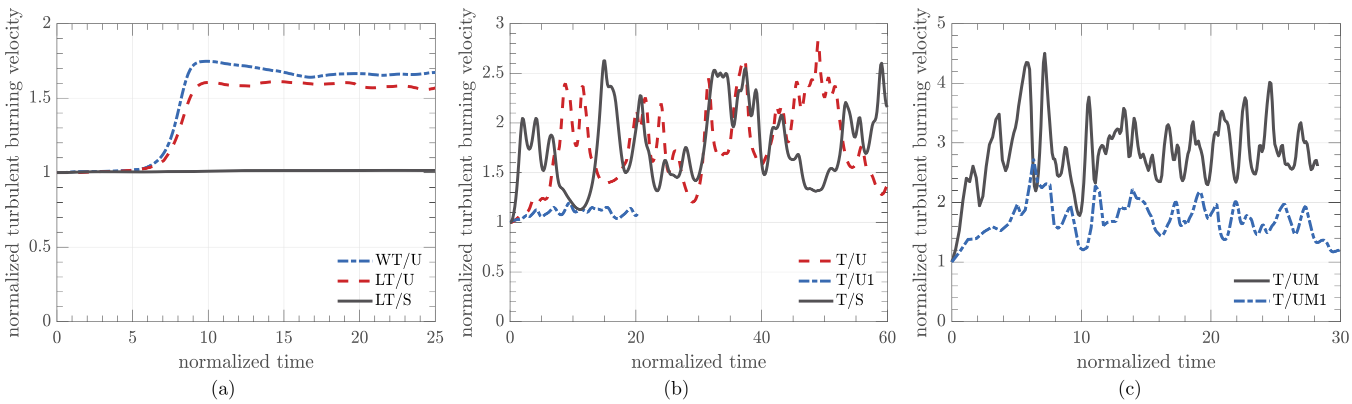

FIG. 3. Evolution of the normalized turbulent burning velocities U_T/S_L in flames (*a*) LT/S (black solid line), LT/U (red dashed line), and WT/U (blue dotted-dashed line), (*b*) T/S (black solid line), T/U (red dashed line), and T/U1 (blue dotted-dashed line). (*c*) T/UM (black solid line), and T/UM1 (blue dotted-dashed line). Time is normalized using the laminar flame time scale τ_f.

burning velocity is increased by turbulence length scale, as reviewed elsewhere [84], see also a recent DNS study by Yu and Lipatnikov [85] or a recent experimental work by Kim *et al.* [86]. To compare magnitudes of these two effects, i.e., (i) an eventual increase in U_T due to TD instability and (ii) an increase in U_T with increasing the length scale L, two more cases T/U1 and T/UM1 (in addition to cases T/U and T/UM, respectively) were run by setting molecular diffusivities D of all species equal to molecular heat diffusivity κ of the mixture. Number one in the names of these two cases shows that the Lewis number $Le = \kappa/D_{H_2} = 1$. In other cases, $Le = 0.32$. Since TD instability does not appear if $Le = 1$ [11], the difference between values of U_T, obtained in cases T/UM1 and T/U1, results from different L in these two cases, i.e., effect (ii). Consequently, a ratio $R1$ of turbulent burning velocities computed in these two cases characterizes magnitude of this effect (an increase in U_T by L). As far as difference between values of U_T obtained in cases T/UM and T/U is concerned, it could also result from TD instability, i.e., effect (i) in addition to effect (ii). Therefore, comparison of a ratio R of burning velocities obtained in cases T/UM and T/U with the ratio $R1$ offers the opportunity to estimate importance of TD instability under conditions when not only perturbations with $k \approx k_n$ (cases LT/S, LT/U, WT/U, T/S, and T/U), but also perturbations with $k \approx k_m$ (case T/UM) and, hence, much higher growth rate $\omega(k)$, see Fig. 2(a), are enabled. Thus, cases T/UM1 and T/U1 were run to estimate contribution $R1$ of effect (ii) to the ratio R computed in cases T/UM and T/U.

III. RESULTS AND DISCUSSION

Computed dependencies of the normalized turbulent burning velocity $U_T(t)/S_L$ on the normalized time t/τ_t are reported in Fig. 3, with representative images of instantaneous turbulent flame surfaces being shown in Figs. 4(c)–4(f). The following trends are worth noting.

First, in case LT/S, the flame surface looks weakly perturbed, see Fig. 4(c), and $U_T(t) \approx S_L$, see curve plotted in black solid line in Fig. 3(a). At the same time, a small increase (less than 10%) in the computational domain width results in significantly increasing flame-surface perturbations, see Fig. 4(d), and turbulent burning velocity, see curve plotted in red dashed line in Fig. 3(a), with the increase in U_T being as large as 60%. Moreover, subsequent increase in u' by about 50% results in weakly increasing (less than 5%) U_T/S_L, see curve plotted in blue dot dashed line in Fig. 3(a). Furthermore, normalized burning velocities obtained from turbulent flames LT/U and WT/U at large t/τ_f are close to burning velocity associated with the nonlinear stage of development of TD instability of the three-dimensional laminar flame in the same computational domain, see curve plotted in yellow solid line in Fig. 2(b). These results indicate that an increase in turbulent burning velocity in cases LT/U and WT/U when compared to case LT/S is mainly controlled by TD instability.

Second, both flame-surface perturbations, cf. Figs. 4(e) and 4(f), and dependencies of $U_T(t)/S_L$, cf. curves plotted in black solid and red dashed lines in Fig. 3(b), look similar in cases T/S and T/U. Since development of TD instability is allowed in case T/U only, these results imply that TD instability weakly affects burning velocities in flames T/S and T/U. Nevertheless, U_T/S_L is significantly higher in low Le flame T/U when compared to counterpart equidiffusive flame T/U1, see curve plotted in blue dot dashed line in Fig. 3(b). This difference indicates that Lewis number substantially affects turbulent burning velocities in the discussed flames despite TD instability does not do so.

Third, comparison of curves plotted in black solid and blue dot dashed lines in Fig. 3(c) shows that differential diffusion results in significantly increasing $U_T(t)/S_L$ in low Le flame T/UM when compared to counterpart equidiffusive flame T/UM1. However, the effect magnitudes are comparable (i) for these two flames (a ratio of mean values of $\overline{U_T}/S_L$, obtained from flames TU/M and TU/M1, is about 1.9, see the far right column in Table I) and (ii) for two flames T/U and T/U1 (the counterpart ratio is about 1.75) despite perturbations with the highest growth rate $\omega_{TD} \approx 0.5\tau_f^{-1}$, see the top red circle in Fig. 2(a), are allowed in the former pair of flames only.

This observation is supported by comparing the ratio $R1 = 1.6$ of $\overline{U_T}$, obtained from equidiffusive flames T/UM1 and T/U1, with the counterpart ratio $R = 1.7$ for low Lewis number flames T/UM and T/U. A weak difference in $R1$ and R implies that the computed increase in U_T with increasing Λ may be attributed to an increase in U_T by the turbulence length

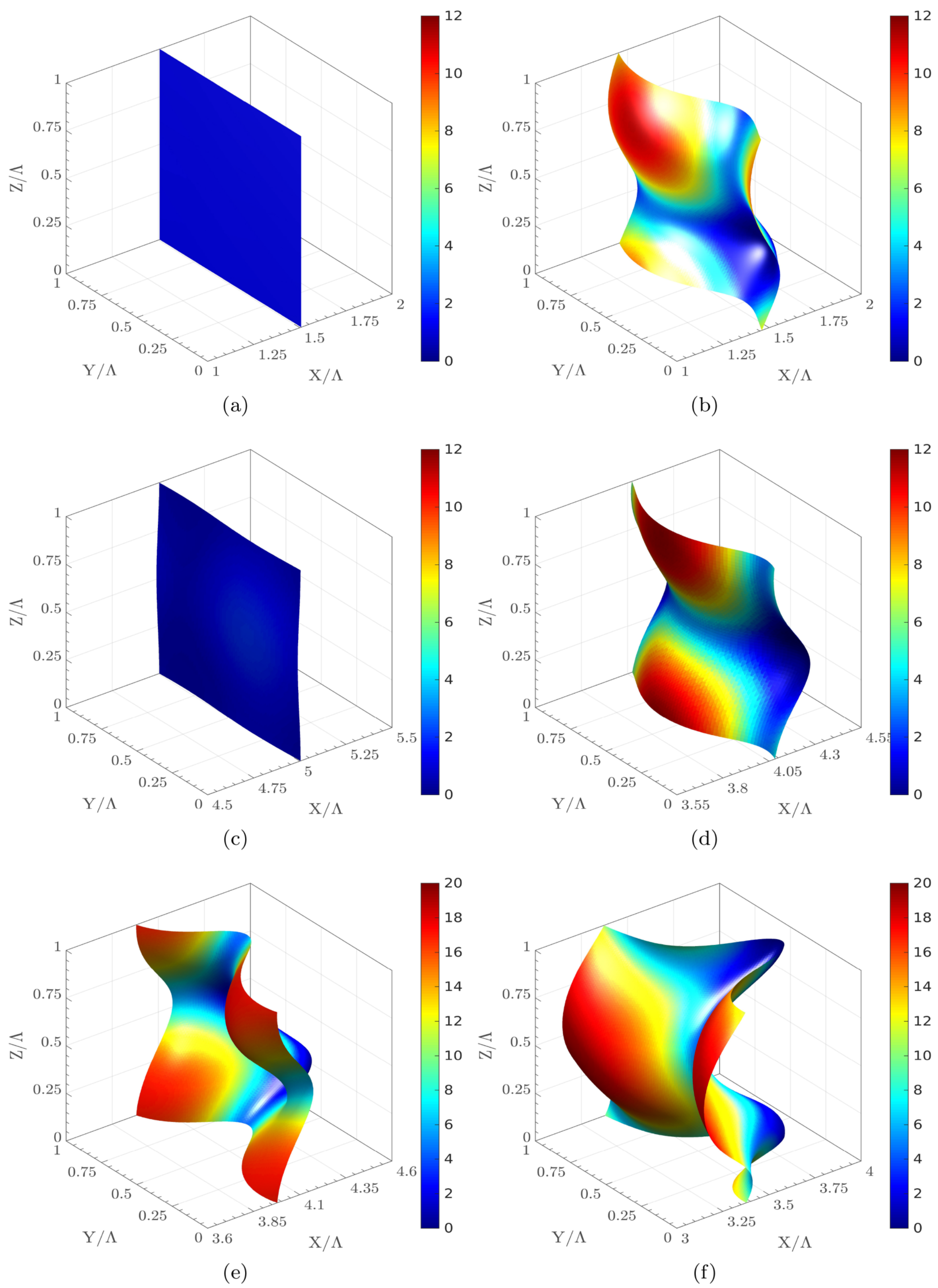

FIG. 4. Images of the instantaneous isosurfaces $c_F(\boldsymbol{x}, t) = 0.5$, with color bars showing the local fuel consumption rate $\dot{\omega}_{H_2}(\boldsymbol{x}, t)$ normalized with the rate $\dot{\omega}_{H_2,L}(c_F = 0.5)$ obtained from the unperturbed laminar flame. (a) stable laminar flame, $\Lambda = 1.26$ mm; (b) unstable laminar flame, $\Lambda = 1.32$ mm; (c) flame LT/S; (d) flame LT/U; (e) flame T/S; and (f) flame T/U.

scale L to the leading order, whereas eventual appearance of perturbations with a high growth rate ω_{TD} plays a minor role in case T/UM.

The reported results indicate that, under the present DNS conditions, TD instability weakly affects turbulent burning velocity at $Ka \geqslant 3.4$ (cases T/UM and T/U). However, the ratio U_T/S_L is controlled by the instability at $Ka = 1.6$ (case WT/U). These numerical findings agree with Eq. (1), which yields $Ka_{TD}^{cr} = 1.9$ if $\tau_f \max\{\omega_{TD}(k)\} \approx 0.5$, see the top red circle in Fig. 2(a). Note that the critical Karlovitz number is substantially less for DL instability [19,53] because $\max\{\omega_{DL}(k)\} < \max\{\omega_{TD}(k)\}$ [49, Fig. 2].

Since development of TD instability is commonly associated with growth of flame surface area, the present results indicating weak contributions of TD instability to U_T in flames T/U and T/UM are in line with earlier DNS [37,75,87] and experimental [29] data, which showed significant (weak) influence of differential diffusion on turbulent burning velocity (flame surface area, respectively). Moreover, the present results are in line with (i) DNS data by Day *et al.* [88], which indicate that both magnitudes and length scales of fuel consumption rate perturbations differ significantly in unstable laminar and turbulent lean hydrogen-air flames, cf. Figs. 6(a) and 6(b) in the cited paper; (ii) DNS data by Berger *et al.* [37], which show significantly different mean local flame characteristics in unstable laminar and moderately turbulent lean H_2-air flames, see Figs. 13, 17, 19-21, 23-25 in the cited paper; and (iii) DNS data by Howarth *et al.* [89], which demonstrate a significant increase in mean local consumption velocity with increasing Ka in lean hydrogen-air flames, see Fig. 20 in the cited paper [the same trend is observed when comparing color scales in Figs. 4(d)-4(f)]. Such DNS data imply that scales and local characteristics of unstable laminar flames are of minor value for predicting the counterpart scales and characteristics of turbulent flames. Furthermore, when discussing DNS data obtained from two V-shaped weakly turbulent ($u'/S_L = 0.72$ and 2.8) flames, Day *et al.* [90, p. 1043] have written that "with increasing turbulence levels fluctuations, at even the lowest intensity levels, appear to suppress to some extent the growth and propagation of the spherical burning cells characteristic of the thermodiffusive instability." Howarth *et al.* [89, p. 15] have also noted that "turbulence is beginning to dominate thermodiffusive effects" at moderate values of Karlovitz number.

Since higher values of U_T obtained from low Le flames T/U and T/UM when compared to their equidiffusive counterparts T/U1 and T/UM1, respectively, do not result from TD instability, this difference in the computed burning velocities requires another explanation. In this regard, leading point concept [8,19], which is based on mathematically rigorous KPP theory [91] of convection-diffusion-reaction equations, see Refs. [92–96] also, appears to be the most promising approach to predicting the significant influence of differential diffusion on turbulent burning velocity, with such effects being documented both experimentally [18,20,29] and numerically [74,97] even in highly turbulent flames. Within the framework of the concept [8], (i) turbulent flame propagation is, in line with the KPP theory, hypothesized to be controlled by reaction zones that advance furthest into fresh reactants (so-called leading points) and (ii) these leading reaction zones are hypothesized to be critically stretched by turbulent eddies, with further stretching of the zones resulting in local combustion quenching (thus, limiting advancement of the zones deeper into the reactants). Accordingly, a critically stretched laminar flame is considered to be a simple model of local burning structures that control flame propagation. In highly stretched laminar flames characterized by a low Le, the local temperature and, hence, burning rate, are well known [3,11] to be significantly increased due to imbalance of molecular fluxes of chemical and thermal energies to and from, respectively, the flame reaction zones. For instance, such an effect is well pronounced in positively curved (curvature center in products) elements of flame surfaces shown in Figs. 4(e) and 4(f) (note that the normalized local fuel consumption rate is as large as 18). Accordingly, substitution of characteristics of unperturbed laminar flames with characteristics of highly stretched laminar flames, which control flame propagation within the framework of leading point concept, offers the opportunity to predict a strong increase in U_T with decreasing Le [3,19] without invoking a hypothesis on TD instability. Further discussion of the concept is beyond the scope of this paper and the reader interested in recent advancements in the concept and its substantiation is referred to articles by Venkateswaran *et al.* [23,25], Kim [98], Zhang *et al.* [26], Dave *et al.* [99], Lipatnikov *et al.* [100], Verma *et al.* [101], Lee *et al.* [70,75,77], Somappa *et al.* [102], Howarth *et al.* [89], and references therein.

IV. CONCLUDING REMARKS

The presented DNS data indicate that the influence of thermodiffusive instability on burning velocity is of primary (secondary) importance in weakly (moderately, respectively) turbulent flames. Under conditions of the present simulations, the instability plays an important role at Karlovitz numbers lower than a critical value, which is of unity order. These DNS results agree with a simple criterion of importance of TD instability in turbulent flames, proposed recently [40].

It is worth bearing in mind that a method adapted to reach the above conclusions required using a narrow computational domain whose width was about $3\delta_L$ in most cases. Accordingly, the reported results could be contaminated by a confinement effect. Such an effect is not expected to reverse the conclusions for the following two reasons. First, TD instability is caused by local variations in burning rate within thin reaction zones and such a small-scale phenomenon should be weakly sensitive to a confinement effect, especially as the domain was sufficiently wide to enable the instability growth. Second, the same major message was delivered when doubling computational domain width (cases T/UM and T/UM1). Nevertheless, more simulations run in wider domains are desirable to confirm the conclusions drawn in the present study. For instance, new simulations could be performed by setting a larger Λ and varying u' around a critical value guessed using Ka_{TD}^{cr}. Such a study is ongoing and results will be reported in a future paper. Another alternative consists in (i) setting sufficiently large Λ and u', (ii) switching off turbulence forcing, and (iii) exploring transition from turbulence-dominated to instability-dominated regime of flame propagation as the turbulence decays. Preliminary results obtained in such simulations [103] are consistent with the conclusions drawn in the present paper.

ACKNOWLEDGMENTS

A.N.L. gratefully acknowledges the financial support by the Chalmers Area of Advance Transport. Other authors have been supported in part by NSFC (Grants No. 91752201, No. 51976088, and No. 92041001), the Shenzhen Science and Technology Program (Grants No. KQTD20180411143441009 and No. JCYJ20210324104802005), Department of Science and Technology of Guangdong Province (Grants No. 2019B21203001 and No. 2020B1212030001), National Science and Technology Major Project (Grants No. J2019-II-0006-0026 and No. J2019-II-0013-0033), and the Center for Computational Science and Engineering of Southern University of Science and Technology.

[1] N. Peters, Multiscale combustion and turbulence, Proc. Combust. Inst. **32**, 1 (2009).

[2] J. F. Driscoll, Turbulent premixed combustion: Flamelet structure and its effect on turbulent burning velocities, Prog. Energy Combust. Sci. **34**, 91 (2008).

[3] A. N. Lipatnikov, *Fundamentals of Premixed Turbulent Combustion* (CRC Press, Boca Raton, FL, 2012).

[4] V. A. Sabelnikov and A. N. Lipatnikov, Recent advances in understanding of thermal expansion effects in premixed turbulent flames, Annu. Rev. Fluid Mech. **49**, 91 (2017).

[5] J. F. Driscoll, J. H. Chen, A. W. Skiba, C. D. Carter, E. R. Hawkes, and H. Wang, Premixed flames subjected to extreme turbulence: Some questions and recent answers, Prog. Energy Combust. Sci. **76**, 100802 (2020).

[6] A. M. Steinberg, P. E. Hamlington, and X. Zhao, Structure and dynamics of highly turbulent premixed combustion, Prog. Energy Combust. Sci. **85**, 100900 (2021).

[7] F. A. Williams, *Combustion Theory*, 2nd ed. (Benjamin/Cummings, Menlo Park, CA, 1985).

[8] V. R. Kuznetsov and V. A. Sabelnikov, *Turbulence and Combustion* (Hemisphere, New York, 1990).

[9] J. Chomiak, *Combustion: A Study in Theory, Fact and Application* (Gordon and Breach, New York, 1990).

[10] N. Peters, *Turbulent Combustion* (Cambridge University Press, Cambridge, UK, 2000).

[11] Ya. B. Zel'dovich, G. I. Barenblatt, V. B. Librovich, and G. M. Makhviladze, *The Mathematical Theory of Combustion and Explosions* (Consultants Bureau, New York, 1985).

[12] L. D. Landau and E. M. Lifshitz, *Fluid Mechanics* (Pergamon Press, Oxford, 1987).

[13] P. Clavin, Dynamical behavior of premixed flame fronts in laminar and turbulent flows, Prog. Energy Combust. Sci. **11**, 1 (1985).

[14] S. Kadowaki and T. Hasegawa, Numerical simulation of dynamics of premixed flames: Flame instability and vortex-flame interaction, Prog. Energy Combust. Sci. **31**, 193 (2005).

[15] M. Matalon, Intrinsic flame instabilities in premixed and nonpremixed combustion, Annu. Rev. Fluid Mech. **39**, 163 (2007).

[16] S. Hochgreb, How fast can we burn, Proc. Combust. Inst. **39**, 2077 (2023).

[17] V. P. Karpov and A. S. Sokolik, Ignition limits in turbulent gas mixtures, Proc. Acad. Sci. USSR, Phys. Chem. **141**, 866 (1961).

[18] V. P. Karpov and E. S. Severin, Effects of molecular-transport coefficients on the rate of turbulent combustion, Combust Explos Shock Waves **16**, 41 (1980).

[19] A. N. Lipatnikov and J. Chomiak, Molecular transport effects on turbulent flame propagation and structure, Prog. Energy Combust. Sci. **31**, 1 (2005).

[20] S. Yang, A. Saha, W. Liang, F. Wu, and C. K. Law, Extreme role of preferential diffusion in turbulent flame propagation, Combust. Flame **188**, 498 (2018).

[21] M. T. Nguyen, D. W. Yu, and S. S. Shy, General correlations of high pressure turbulent burning velocities with the consideration of Lewis number effect, Proc. Combust. Inst. **37**, 2391 (2019).

[22] A. N. Lipatnikov, Y.-R. Chen, and S. S. Shy, An experimental study of the influence of Lewis number on turbulent flame speed at different pressures, Proc. Combust. Inst. **39**, 2339 (2023).

[23] P. Venkateswaran, A. Marshall, D. H. Shin, D. Noble, J. Seitzman, and T. Lieuwen, Measurements and analysis of turbulent consumption speeds of H_2/CO mixtures, Combust. Flame **158**, 1602 (2011).

[24] S. Daniele, P. Jansohn, J. Mantzaras, and K. Boulouchos, Turbulent flame speed for syngas at gas turbine relevant conditions, Proc. Combust. Inst. **33**, 2937 (2011).

[25] P. Venkateswaran, A. Marshall, J. Seitzman, and T. Lieuwen, Pressure and fuel effects on turbulent consumption speeds of H_2/CO blends, Proc. Combust. Inst. **34**, 1527 (2013).

[26] W. Zhang, J. Wang, Q. Yu, W. Jin, M. Zhang, and Z. Huang, Investigation of the fuel effects on burning velocity and flame structure of turbulent premixed flames based on leading points concept, Combust. Sci. Technol. **190**, 1354 (2018).

[27] Y. Xia, G. Hashimoto, K. Hadi, N. Hashimoto, A. Hayakawa, H. Kobayashi, and O. Fujita, Turbulent burning velocity of ammonia/oxygen/nitrogen premixed flame in O_2-enriched air condition, Fuel **268**, 117383 (2020).

[28] C. Lhuillier, P. Brequigny, F. Contino, and C. Mounaim-Rousselle, Experimental investigation on ammonia combustion behavior in a spark-ignition engine by means of laminar and turbulent expanding flames, Proc. Combust. Inst. **38**, 5859 (2021).

[29] X. Cai, Q. Fan, X.-S. Bai, J. Wang, M. Zhang, Z. Huang, M. Aldén, and Z. Li, Turbulent burning velocity and its related statistics of ammonia-hydrogen-air jet flames at high Karlovitz number: Effect of differential diffusion, Proc. Combust. Inst. **39**, 4215 (2023).

[30] S. Wang, A. M. Elbaz, O. Z. Arab, and W. L. Roberts, Turbulent flame speed measurement of NH_3/H_2/air and CH_4/air flames and a numerical case study of NO emission in a constant volume combustion chamber, Fuel **332**, 126152 (2023).

[31] S. Wang, A. M. Elbaz, G. Wang, Z. Wang, and W. L. Roberts, Turbulent flame speed of $NH_3/CH_4/H_2/H_2O$/air-mixtures: Effects of elevated pressure and Lewis number, Combust. Flame **247**, 112488 (2023).

[32] A. J. Aspden, M. S. Day, and J. B. Bell, Turbulence-flame interactions in lean premixed hydrogen: Transition to the distributed burning regime, J. Fluid Mech. **680**, 287 (2011).

[33] N. Chakraborty and R. S. Cant, Effects of Lewis number on flame surface density transport in turbulent premixed combustion, Combust. Flame **158**, 1768 (2011).

[34] H. Kobayashi, Y. Otawara, J. Wang, F. Matsuno, Y. Ogami, M. Okuyama, T. Kudo, and S. Kadowaki, Turbulent premixed flame characteristics of a $CO/H_2/O_2$ mixture highly diluted with CO_2 in a high-pressure environment, Proc. Combust. Inst. **34**, 1437 (2013).

[35] C. Dopazo, L. Cifuentes, and N. Chakraborty, Vorticity budgets in premixed combusting turbulent flows at different Lewis numbers, Phys. Fluids **29**, 045106 (2017).

[36] M. Zhang, J. Wang, and Z. Huang, Turbulent flame structure characteristics of hydrogen enriched natural gas with CO_2 dilution, Int. J. Hydrog. Energy **45**, 20426 (2020).

[37] L. Berger, A. Attili, and H. Pitsch, Synergistic interactions of thermodiffusive instabilities and turbulence in lean hydrogen flames, Combust. Flame **244**, 112254 (2022).

[38] D. Bradley, A. K. C. Lau, and M. Lawes, Flame stretch rate as a determinant of turbulent burning velocity, Phil. Trans. R. Soc. Lond. A **338**, 359 (1992).

[39] V. P. Karpov, A. N. Lipatnikov, and V. L. Zimont, A test of an engineering model of premixed turbulent combustion, Symp. Int. Combust. **26**, 249 (1996).

[40] J. Chomiak and A. N. Lipatnikov, A simple criterion of importance of thermo-diffusive instability in premixed turbulent flames, Phys. Rev. E **107**, 015102 (2023).

[41] J. D. Buckmaster and G. S. S. Ludford, *Theory of Laminar Flames* (Cambridge Univ. Press, Cambridge, UK, 1982).

[42] G. I. Sivashinsky, C. K. Law, and G. Joulin, On stability of premixed flames in stagnation-point flow, Combust. Sci. Technol. **28**, 155 (1982).

[43] Y. Kortsarts, J. Brailovsky, and G. I. Sivashinsky, On hydrodynamic instability of stretched flames, Combust. Sci. Technol. **123**, 207 (1997).

[44] C. Altantzis, C. E. Frouzakis, A. G. Tomboulides, K. Kerkemeier, and K. Boulouchos, Detailed numerical simulations of intrinsically unstable two-dimensional planar lean premixed hydrogen/air flames, Proc. Combust. Inst. **33**, 1261 (2011).

[45] C. Altantzis, C. E. Frouzakis, A. G. Tomboulides, M. Matalon, and K. Boulouchos, Hydrodynamic and thermodiffusive instability effects on the evolution of laminar planar lean premixed hydrogen flames, J. Fluid Mech. **700**, 329 (2012).

[46] C. E. Frouzakis, N. Fogla, A. G. Tomboulides, C. Altantzis, and M. Matalon, Numerical study of unstable hydrogen/air flames: Shape and propagation speed, Proc. Combust. Inst. **35**, 1087 (2015).

[47] L. Berger, K. Kleinheinz, A. Attili, and H. Pitsch, Characteristic patterns of thermodiffusively unstable premixed lean hydrogen flames, Proc. Combust. Inst. **37**, 1879 (2019).

[48] L. Berger, A. Attili, and H. Pitsch, Intrinsic instabilities in premixed hydrogen flames: Parametric variation of pressure, equivalence ratio, and temperature, Part 1 - Dispersion relations in the linear regime, Combust. Flame **240**, 111935 (2022).

[49] L. Berger, M. Grinberg, B. Jürgens, P. E. Lapenna, F. Creta, A. Attili, and H. Pitsch, Flame fingers and interactions of hydrodynamic and thermodiffusive instabilities in laminar lean hydrogen flames, Proc. Combust. Inst. (to be published)

[50] A. S. Monin and A. M. Yaglom, *Statistical Fluid Mechanics: Mechanics of Turbulence*, Vol. 2 (The MIT Press, Cambridge, MA, 1975).

[51] U. Frisch, *Turbulence. The Legacy of A. N. Kolmogorov* (Cambridge University Press, Cambridge, UK, 1995).

[52] H. Boughanem and A. Trouvé, The domain of influence of flame instabilities in turbulent premixed combustion, Symp. Int. Combust. **27**, 971 (1998).

[53] S. Chaudhuri, V. Akkerman, and C. K. Law, Spectral formulation of turbulent flame speed with consideration of hydrodynamic instability, Phys. Rev. E **84**, 026322 (2011).

[54] F. Creta and M. Matalon, Propagation of wrinkled turbulent flames in the context of hydrodynamic theory, J. Fluid Mech. **680**, 225 (2011).

[55] N. Fogla, F. Creta, and M. Matalon, Influence of the Darrieus-Landau instability on the propagation of planar turbulent flames, Proc. Combust. Inst. **34**, 1509 (2013).

[56] N. Fogla, F. Creta, and M. Matalon, Effect of folds and pockets on the topology and propagation of premixed turbulent flames, Combust. Flame **162**, 2758 (2015).

[57] N. Fogla, F. Creta, and M. Matalon, The turbulent flame speed for low-to-moderate turbulence intensities: Hydrodynamic theory vs. experiments, Combust. Flame **175**, 155 (2017).

[58] S. Yang, A. Saha, Z. Liu, and C. K. Law, Role of Darrieus-Landau instability in propagation of expanding turbulent flames, J. Fluid Mech. **850**, 784 (2018).

[59] P. E. Lapenna, G. Troiani, R. Lamioni, and F. Creta, Mitigation of Darrieus-Landau instability effects on turbulent premixed flames, Proc. Combust. Inst. **38**, 2885 (2021).

[60] P. Pelcé and P. Clavin, Influence of hydrodynamics and diffusion upon the stability limits of laminar premixed flames, J. Fluid Mech. **124**, 219 (1982).

[61] M. Matalon and B. J. Matkowsky, Flames as gas dynamic discontinuities, J. Fluid Mech. **124**, 239 (1982).

[62] M. L. Frankel and G. J. Sivashinsky, The effect of viscosity on hydrodynamic stability of a plane flame front, Combust. Sci. Technol. **29**, 207 (1982).

[63] A. G. Class, B. J. Matkowsky, and A. Y. Klimenko, Stability of planar flames as gasdynamic discontinuities, J. Fluid Mech. **491**, 51 (2003).

[64] A. P. Kelley, J. K. Bechtold, and C. K. Law, Premixed flame propagation in a confining vessel with weak pressure rise, J. Fluid Mech. **691**, 26 (2012).

[65] C. Clanet and G. Searby, First Experimental Study of the Darrieus-Landau Instability, Phys. Rev. Lett. **80**, 3867 (1998).

[66] J.-M. Truffaut and G. Searby, Experimental study of the Darrieus-Landau instability on an inverted-V flame, and measurement of the Markstein number, Combust. Sci. Technol. **149**, 35 (1999).

[67] R. Yu, X.-S. Bai, and V. Bychkov, Fractal flame structure due to the hydrodynamic Darrieus-Landau instability, Phys. Rev. E **92**, 063028 (2015).

[68] F. Creta, P. E. Lapenna, R. Lamioni, N. Fogla, and M. Matalon, Propagation of premixed flames in the presence of Darrieus-Landau and thermal diffusive instabilities, Combust. Flame **216**, 256 (2020).

[69] L. Berger, A. Attili, and H. Pitsch, Intrinsic instabilities in premixed hydrogen flames: Parametric variation of pressure, equivalence ratio, and temperature, Part 2 - Non-linear regime and flame speed enhancement, Combust. Flame **240**, 111936 (2022).

[70] H. C. Lee, P. Dai, M. Wan, and A. N. Lipatnikov, Influence of molecular transport on burning rate and conditioned species concentrations in highly turbulent premixed flames, J. Fluid Mech. **928**, A5 (2021).

[71] H. C. Lee, X. Liu, P. Dai, Z. Chen, A. Abdelsamie, M. Wan, Effects of Lewis and Karlovitz numbers on transport equations for turbulent kinetic energy and enstrophy, Acta Mech. Sin. **38**, 121573 (2022).

[72] H. C. Lee, P. Dai, M. Wan, and A. N. Lipatnikov, A DNS study of extreme and leading points in lean hydrogen-air turbulent flames - part I: Local thermochemical structure and reaction rates, Combust. Flame **235**, 111716 (2022).

[73] H. C. Lee, P. Dai, M. Wan, and A. N. Lipatnikov, A DNS study of extreme and leading points in lean hydrogen-air turbulent flames - part II: Local velocity field and flame topology, Combust. Flame **235**, 111712 (2022).

[74] H. C. Lee, P. Dai, M. Wan, and A. N. Lipatnikov, Lewis number and preferential diffusion effects in lean hydrogen-air highly turbulent flames, Phys. Fluids **34**, 035131 (2022).

[75] H. C. Lee, P. Dai, M. Wan, and A. N. Lipatnikov, A numerical support of leading point concept, Int. J. Hydrog. Energy **47**, 23444 (2022).

[76] H. C. Lee, A. Abdelsamie, P. Dai, M. Wan, and A. N. Lipatnikov, Influence of equivalence ratio on turbulent burning velocity and extreme fuel consumption rate in lean hydrogen-air turbulent flames, Fuel **327**, 124969 (2022).

[77] H. C. Lee, P. Dai, M. Wan, and A. N. Lipatnikov, Displacement speed, flame surface density, and burning rate in highly turbulent premixed flames characterized by low Lewis numbers, J. Fluid Mech. **961**, A21 (2023).

[78] A. Kéromnès, W. K. Metcalfe, K. A. Heufer, N. Donohoe, A. K. Das, C.-J. Sung, J. Herzler, C. Naumann, P. Griebel, O. Mathieu, M. C. Krejci, E. L. Petersen, W. J. Pitz, and H. J. Curran, An experimental and detailed chemical kinetic modeling study of hydrogen and syngas mixture oxidation at elevated pressures, Combust. Flame **160**, 995 (2013).

[79] D. Goodwin, N. Malaya, H. Moffat, and R. Speth, *Cantera: An object-oriented software toolkit for chemical kinetics, thermodynamics, and transport processes* (Caltech, Pasadena, CA, 2009).

[80] A. Abdelsamie, G. Fru, T. Oster, F. Dietzsch, G. Janiga, and D. Thévenin, Towards direct numerical simulations of low-Mach number turbulent reacting and two-phase flows using immersed boundaries, Comput. Fluids **131**, 123 (2016).

[81] T. Lundgren, Linearly forced isotropic turbulence (Tech. Rep., Minnesota University of Minneapolis, 2003).

[82] C. Rosales and C. Meneveau, Linear forcing in numerical simulations of isotropic turbulence: Physical space implementations and convergence properties, Phys. Fluids **17**, 095106 (2005).

[83] P. L. Carroll and G. Blanquart, The effect of velocity field forcing techniques on the Karman-Howarth equation, J. Turbul. **15**, 429 (2014).

[84] A. N. Lipatnikov and J. Chomiak, Turbulent flame speed and thickness: phenomenology, evaluation, and application in multi-dimensional simulations, Prog. Energy Combust. Sci. **28**, 1 (2002).

[85] R. Yu and A. N. Lipatnikov, DNS study of dependence of bulk consumption velocity in a constant-density reacting flow on turbulence and mixture characteristics, Phys. Fluids **29**, 065116 (2017).

[86] J. Kim, A. Satija, R. P. Lucht, and J. P. Gore, Effects of turbulent flow regime on perforated plate stabilized piloted lean premixed flames, Combust. Flame **211**, 158 (2020).

[87] N. Chakraborty, I. Konstantinou, and A. N. Lipatnikov, Effects of Lewis number on vorticity and enstrophy transport in turbulent premixed flames, Phys. Fluids **28**, 015109 (2016).

[88] M. S. Day, J. B. Bell, R. K. Cheng, S. Tachibana, V. E. Beckner, and M. J. Lijewski, Cellular burning in lean premixed turbulent hydrogen-air flames: coupling experimental and computational analysis at the laboratory scale, J. Phys.: Conf. Ser. **180**, 012031 (2009).

[89] T. L. Howarth, E. F. Hunt, and A. J. Aspden, Thermodiffusively-unstable lean premixed hydrogen flames: Phenomenology, empirical modelling, and thermal leading points, Combust. Flame **253**, 112811 (2023).

[90] M. S. Day, J. B. Bell, P. T. Bremer, V. Pascucci, V. E. Beckner, and M. J. Lijewski, Turbulence effects on cellular burning structures in lean premixed hydrogen flames, Combust. Flame **156**, 1035 (2009).

[91] A. N. Kolmogorov, E. G. Petrovsky, and N. S. Piskounov, A study of the diffusion equation with a source term and its application to a biological problem, Bjul. MGU Section A **1**, 1 (1937).

[92] U. Ebert and W. van Saarlos, Front propagation into unstable states: universal algebraic convergence towards uniformly translating pulled fronts, Physica D **146**, 1 (2000).

[93] W. Vansaarloos, Front propagation into unstable states, Phys. Rep. **386**, 29 (2003).

[94] V. A. Sabelnikov and A. N. Lipatnikov, Transition from pulled to pushed premixed turbulent flames due to countergradient transport, Combust. Theory Model. **17**, 1154 (2013).

[95] V. A. Sabelnikov and A. N. Lipatnikov, Transition from pulled to pushed fronts in premixed turbulent combustion: theoretical and numerical study, Combust. Flame **162**, 2893 (2015).

[96] V. A. Sabelnikov, N. N. Petrova, and A. N. Lipatnikov, Analytical and numerical study of travelling waves using the Maxwell-Cattaneo relaxation model extended to reaction-advection-diffusion systems, Phys. Rev. E **94**, 042218 (2016).

[97] A. J. Aspden, M. S. Day, and J. B. Bell, Towards the distributed burning regime in turbulent premixed flames, J. Fluid Mech. **871**, 1 (2019).

[98] S. H. Kim, Leading points and heat release effects in turbulent premixed flames, Proc. Combust. Inst. **36**, 2017 (2017).

[99] H. L. Dave, A. Mohan, and S. Chaudhuri, Genesis and evolution of premixed flames in turbulence, Combust. Flame **196**, 386 (2018).

[100] A. N. Lipatnikov, N. Chakraborty, and V. A. Sabelnikov, Transport equations for reaction rate in laminar and turbulent premixed flames characterized by non-unity Lewis number, Int. J. Hydrog. Energy **43**, 21060 (2018).

[101] S. Verma, F. Monnier, and A. N. Lipatnikov, Validation of leading point concept in RANS simulations of highly turbulent lean syngas-air flames with well-pronounced diffusional-thermal effects, Int. J. Hydrog. Energy **46**, 9222 (2021).

[102] S. Somappa, V. Acharia, and T. Lieuwen, Finite flame thickness effects on KPP turbulent burning velocities, Phys. Rev. E **106**, 055107 (2022).

[103] H. C. Lee, P. Dai, M. Wan, V. A. Sabelnikov, and A. N. Lipatnikov, Transition from turbulence-dominated to instability-dominated combustion regime in lean hydrogen-air flames, arXiv:2303.07057.